Climate Dynamics (2023) 60:1523–1541
https://doi.org/10.1007/s00382-022-06376-0

Snow depth and snow cover over the Tibetan Plateau observed from space in against ERA5: matters of scale

Yonghui Lei[1] · Jinmei Pan[1] · Chuan Xiong[2] · Lingmei Jiang[3] · Jiancheng Shi[4]

Received: 20 September 2021 / Accepted: 2 June 2022 / Published online: 9 July 2022

Abstract
There has been a statement that the satellite and reanalyses significantly overestimate snow depths (SDs) as compared with in-situ observations over the Tibetan Plateau (TP). The inconsistency may be partly due to representations related to different spatial resolutions. To further clarify matters of scale, this work estimates and compares the fractional snow cover (FSC) from MODIS (500 m), SDs from Sentinel-1 C-band SAR (1 km), ERA5-Land (9 km) and ERA5 (31 km), together with ground observations from GHCN-D and at 6 newly-established stations in the Namco watershed. SD and FSC from MERRA-2 (50 km) are also discussed in comparison with ERA5s. Results indicate that SD from fine resolution reanalysis has better consistency to in-situ observations over the TP. SD of ERA5-Land matches in-situ measurements better than ERA5 and MERRA-2. Overestimates of SDs in reanalyses are likely for shallow snowpack. However, underestimates are found for deep snow particularly late in the snow season. Improvements are displayed in ERA5-Land, while increased SD is attributed by altitude in fine resolution. Overall SDs of ERA5 and ERA5-Land have similar spatial distributions and annual cycle patterns over the TP, consistent with satellite-based datasets. A notable defect of ERA5s is related to delayed ablation of deep snowpack during spring and early summer. It causes cold temperature biases at surface that may impact on the land-atmosphere interaction. Snow analysis that combines the information of FSC into SD has been demonstrated in MERRA-2 data. Snow analysis has the potential to improve SDs of ERA5s over the TP.

Keywords Snow depth · Snow cover · Remote sensing · Reanalysis data

1 Introduction

The snowpack and its properties (e.g., snow cover duration and extent, snow mass, snow albedo) play an important role in the climate system (Cohen 1994; Zhang 2005). The high albedo and good thermal insulation of snow lead to unique interactions between the land surface and lower atmosphere. The snow covered area with high albedo reflects more solar radiation compared with the snow-free land. Fresh snow can reflect up to 90% of incoming solar radiation. As snow ages, its density increases and its albedo decreases. The insulating property of snow affects the energy exchange between surface and atmosphere. Even a few decimeters of snow cover can prevent the soil freezing, and slow down the ablation of glaciers and ice sheets. The insulating effect increases with the snow depth. The snowmelt affects soil moisture, evapotranspiration, and runoff, playing a critical role in water resources (Bormann et al. 2018).

The Tibetan Plateau (TP) comprises the highest mountains, including the Pamir, Karakoram, Kunlun, Himalaya, Nyainqentanglha, Tanggula, Hengduan and Qilian chains, which feed the major rivers in Asia. Snowpack plays a critical role in the mountain environment. The annual mean temperature across the TP is generally below 0 °C (Frauenfeld et al. 2005). The dominant atmospheric circulations (including

✉ Yonghui Lei
yonghui.lei@hotmail.com

1 State Key Laboratory of Remote Sensing Science, Aerospace Information Research Institute of Chinese Academy of Sciences, Beijing Normal University, Jia No. 20 North Datun Road, Chaoyang District, 100101 Beijing, China

2 Faculty of Geosciences and Environmental Engineering, Southwest Jiaotong University, 610031 Chengdu, China

3 State Key Laboratory of Remote Sensing Science, Jointly Sponsored by Beijing Normal University and Aerospace Information Research Institute of Chinese Academy of Sciences, 100875 Beijing, China

4 National Space Science Center, Chinese Academy of Sciences, 100101 Beijing, China

the Indian monsoon, the East Asian monsoon and the westerly jet stream) primarily influence the TP by interactions of climate patterns like El Nino-Southern Oscillation (ENSO), North Atlantic Oscillation (NAO), and Pacific Decadal Oscillation (PDO) (Wu et al. 2015; Yao et al. 2019; Liu et al. 2020). Snowfall is frequent in the southern and western edges where moisture from the westerlies and Indian monsoon spills over the frontier ranges. Snowfall occurs frequently in the southeast where the water vapor from the south is channeled up through the Yarlung Zangbo valley. In contrast, most of the interior of the TP has infrequent snowfall due to the blocking effect of the Himalaya and Karakoram mountains. In addition, the strong solar radiation and low air humidity are unfavorable factors for the snow accumulation. As a result, shallow, patchy and transient snowpack is prominent over the TP (Pu and Xu 2009).

The accurate representation of times and locations of the short-lived snowpack is vital to the hydrological cycle and water availability in the context of global warming. The relatively thin snow is highly sensitive to climate change especially in the TP. It can exert major control on the atmospheric circulation at the regional and global scales. There is a significant warming trend over the TP during the recent decades (Duan et al. 2006; Duan and Xiao 2015).

The uncertainty in variability of snow is large over the TP (Jiang et al. 2020; Yan et al. 2022; Liu et al. 2021). Various results of the snow change could depend on regions, studied data sources and periods, methods of investigation and so on (You et al. 2020; Xu et al. 2017; Bian et al. 2020).

Three kinds of snow data sources (meteorological stations, satellite remote sensing and model-based estimates) are available over the TP (Basang et al. 2017). There are over 100 in-situ observations providing measurements of snow depth, but most stations are located in the eastern TP. Few stations in the western TP and/or in the higher mountains with extensive snow impede the understanding of snow changes.

Compared to the ground-based measurements, satellite observations and modeling data have better spatial coverage. The snow extent is monitored by optical satellites. For example, NASA's Moderate-resolution Imaging Spectroradiometer (MODIS) can provide daily, 500-m globally binary or fractional snow cover (FSC) since February 2000 (Hall et al. 2002). Snow water equivalent (SWE) and snow depth (SD) can be monitored by passive microwave satellites, but their coarse resolution (~ 25 km) limits their application in mountains (Dozier et al. 2016; Dai et al. 2018; Bian et al. 2019). NOAA has provided a multi-sensor snow cover product (the Interactive Multi-sensor Snow and Ice Mapping System, IMS) at a high resolution by blending the optical and infrared data with the microwave data. Some alternative remote sensing techniques have been developed to fill the mountain snow observation gaps (Bormann et al. 2018; Painter et al. 2016). Sentinel-1 snow depth retrievals are ~ weekly at 1 km resolution, which successfully captured the spatial variability between and within mountain ranges and the inter-annual differences in the US Sierra Nevada and European Alps (Lievens et al. 2019).

Model-based reanalyses provide another approach with essential information of snow in weather and climate studies. Atmospheric and land reanalyses provide simulated snow temperature, snow albedo, snow density, SWE and SD by assimilating in-situ, ballon-borne and satellite observations in forecast models or initializing land surface models. Previous studies suggested contradictory performances of reanalyses over different regions. The broad features of SD over the plains of central and northern Russia were realistically reproduced (Wegmann et al. 2017). However, validations of SWE/SD in several reanalyses were reported to have a systematic overestimation over the TP (Orsolini et al. 2019; Bian et al. 2019). Uncertainties come from different land surface schemes or models, input data, or assimilation systems. Overestimates were also attributed to common precipitation bias in models. A recent work evaluated SD fields derived from the European Centre for Medium-Range Weather Forecasts (ECMWF) products including both climate reanalyses (ERA5 and ERA-Interim) and the land component (ERA5-Land) (Muñoz-Sabater et al. 2021). They found that SD estimates from ERA5 match measurements slightly better at the highest mountains compared to ERA-Interim and ERA5-Land.

Nevertheless, inter-comparison discrepancy of snow states and changes over the TP may come from inconsistent spatial resolution and elevations between in situ observations and gridded reanalyses data (Bian et al. 2019; Liu et al. 2021; Yan et al. 2022). Accurate snow data with higher spatial resolutions are essential for mountainous region. The optical-based FSC was widely used in previous studies, though daily data can be affected by cloud coverage. Fine-scale SD or SWE data over a large domain over the TP remain a great challenge. A few studies had tried to improve snow mass data at higher resolutions (Yan et al. 2022; Liu et al. 2021; Wang et al. 2020a, c). The approach is to blend the coarse resolution snow mass datasets and other auxiliary datasets with higher spatial resolutions. The optical-based FSC is preferable to a spatial-temporal downscaling of SD (Yan et al. 2022).

In this work, investigation focuses on matters of scale in representation of snowpack over the TP with datasets ranging from fine to coarse resolutions. Because the relative paucity of measurements in High Mountain Asia (HMA) precludes confident representation of snow properties, remote sensing and model-derived reanalysis datasets are critical. FSC derived from MODIS provides fine-scale

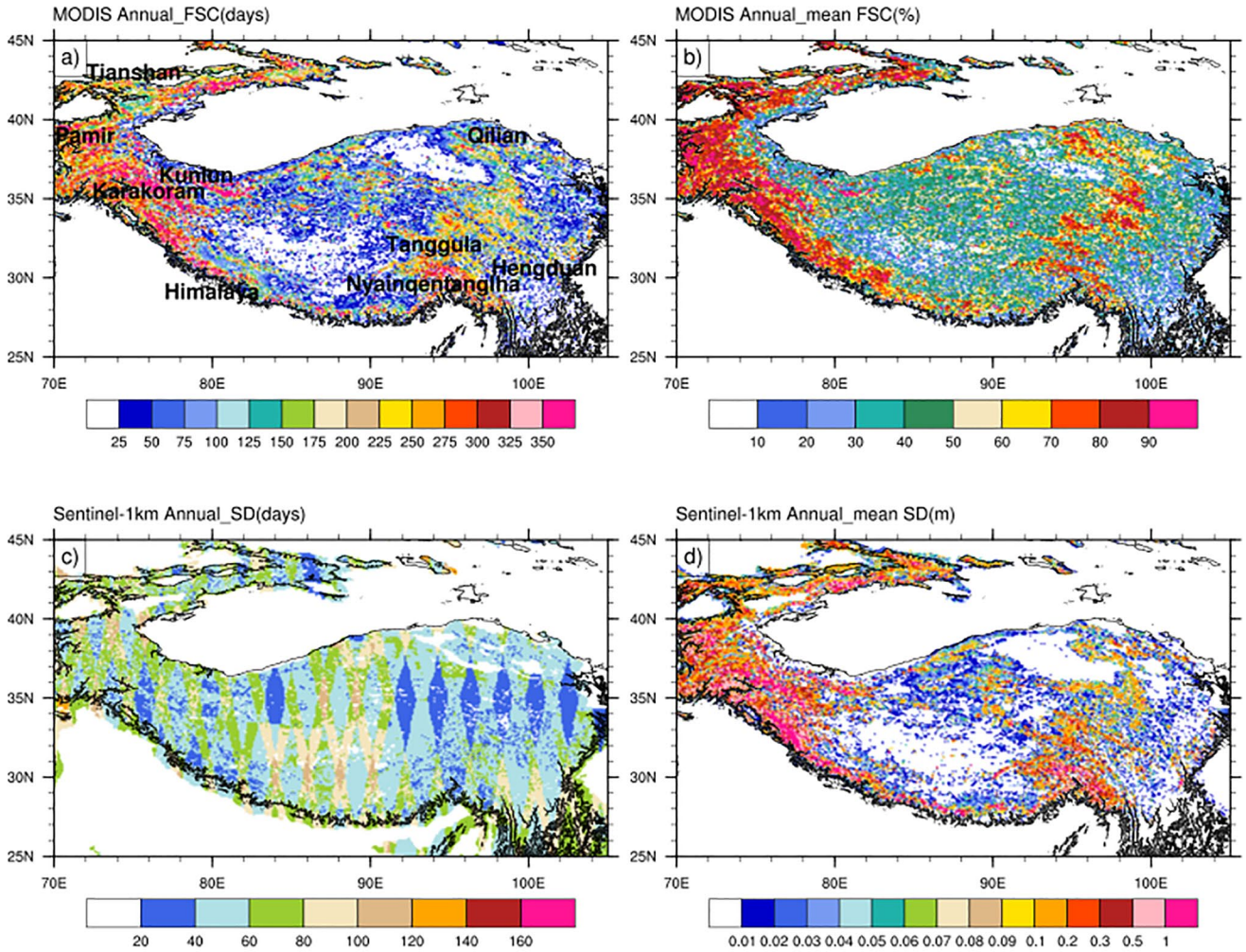

Fig. 1 Main mountains and study domain–Tibetan Plateau (TP) is outlined by the 2000 m DEM contour. MODIS (500 m) FSC and Sentinel (1 km) SD data during September 2018 to August 2019 are investigated. (a) and (b) are days with snow cover presence and averaged FSC derived by MODIS; (c) and (d) are days with Sentinel-1 backscatter measurements and corresponding the averaged SD, respectively

information for snow states and changes. SD derived from Sentinel-1 and reanalyses of ERA5 and ERA5-land are used extensively to examine over the TP in this study. The aim of this study is to demonstrate the capability and limitation of different datasets, including MODIS FSC retrievals, Sentinel-1 SD retrievals, simulated SDs of ERA5 and ERA5-Land in representation of snowpack over the TP.

2 Data and methods

The study domain and the major mountain ranges are shown in Fig. 1. The TP is located in the domain of 25–45°N and 70–105°E, with the focus on the elevation above 2000 m. The snow hydrological year was defined as September 1 to August 31 of the following year because the seasonal cycle of the SD over the TP indicates the lowest amount in September (Yan et al. 2022). Averaged FSC and SD derived from the highest resolutions of available remote sensing (MODIS 500 m and Sentinel-1 1 km) during one snow year (2018/2019) are shown in Fig. 1. Although uncertainties exist, these are the best general pictures for snow states over the HMA domain. Spatial distributions of FSC and SD highlight differences between mountains and the interior TP.

Daily ground measurements of precipitation and SD are used as the "true" values for assessing the accuracy of the gridded FSC and SD derived from satellites. SDs derived from ERA5-Land (9 km) and ERA5 (31 km) are compared with in-situ and satellite-based datasets. Matters of scale are revealed with datasets ranging from fine to coarse resolutions. Details of used data are introduced below.

2.1 MODIS FSC retrieval (MODAGE, daily and 500 m resolution)

The MODAGE data (Hao et al. 2019) is utilized to address the status and changes in fine scales (daily, 500 m) of FSC over the TP during 2017–2020 in this study. The previous study indicated that MODAGE snow cover data is better performed over the TP. MOD10A1 and MYD10A1 provided by the NASA National Snow and Ice Data Center were affected by the snow cover's patchiness, local illumination angle and vegetation background (Shi 2012). MOD10A1 retrievals utilized a universal regression relationship to calculate the global FSC based on the NDSI (Normalized-Difference Snow Index), which are less suitable over the TP. MODAGE is based on the linear spectral mixture method that is also used in the updated NASA snow product MODSCAG. MODAGE was able to characterize snow states over the TP (Hao et al. 2019).

MODAGE was retrieved from MOD09GA (Version 6), and the cloud mask file was also extracted from MOD09GA (Hao et al. 2019). MODAGE also utilizes the algorithm of multiple endmember spectral mixture analysis, but conducts a method of automatic endmember extraction (Shi 2012). Cloud removal procedures were developed by utilizing temporal linear interpolation within one month window. Afterwards, spatial weighted square revised distance spatial interpolation. Previous evaluation had confirmed that MODAGE produced smaller root mean square errors (RMSE) than MOD10A1 (Hao et al. 2019).

2.2 SD derived from Sentinel-1 (1-km)

The Sentinel-1 snow depth retrievals over the Northern Hemisphere mountain ranges is based on an empirical change detection approach to capture C-band cross-polarized backscatter signature over snow (Lievens et al. 2019). The retrieval algorithm used snow cover absence/presence observations derived from IMS dataset as auxiliary input. Evaluation with measurements from ~4000 sites mostly in the western US and Europe demonstrated the effectiveness of the Sentinel-1 retrievals to capture the overall spatial variability of SD. In this work, the performance of Sentinel-1 is evaluated over the TP where shallow snow is prominent apart from the west and southeast.

The Sentinel-1 snow depth retrievals are available online at https://ees.kuleuven.be/project/c-snow. SD retrievals are available over the TP in the period 2017 through March 2020, which provide satellite-based estimates for comparisons in this study. Figure 1c shows the number (N; dimensionless) of Sentinel-1 backscatter measurements for one snow year (2018/2019) when the SD retrievals are relatively complete. N is calculated after combining the ascending and descending measurements at the daily timescales. SD retrievals are on average available every ~4 days and ~2 weeks over the TP. Although uneven samples may affect results of analysis, Sentinel-1 is capable to capture spatial variability of SD over the large domain of TP (Fig. 1d). Deeper SD is consistent with more days and larger fractions of snow cover over mountainous areas. Averaged SD is over 10 cm over the mountains, while it is less than 1–2 cm over the interior TP.

2.3 Ground measurements of precipitation and SD

The daily precipitation data during 2018–2019 observed at 91 meteorological stations of the China Meteorological Administration (CMA) are used as auxiliary data to assess the rationality of the gridded FSC and SD. The Global Historical Climatology Network Daily database (GHCN-D) provides direct measurements of SD, which is free for public access to the most recent observations (Menne et al. 2012). There are 30 sites providing observational SD (> 1 cm) from 2017 to 2020. Total measurements of SD at these 30 ground stations range from less than 10 to over 300 times corresponding to valid data in retrievals of Sentinel-1(Fig. 2a).

An intensive observational experiment was organized in June 2019, in a collaboration of the State Key Laboratory of Remote Sensing Science of Aerospace Information Research Institute, Institute of Tibetan Plateau Research and Tsinghua University. A network of 6 ground stations (Fig. 2b) was built near the Namco (called precipitation-snowpack multi-source observation platform, PSMOP-Namco). SD was recorded every 10 min in the period July 2019-June 2020, together with temperatures at the lower atmosphere (1.5 m above the surface, Ta) and the 5 cm soil (Ts).

Daily SD in-situ observations at these 36 stations (GHCN-D and PSMOP-Namco) are "true" values in this study. Ground measurements are mostly distributed to the northwest and eastern TP. SD provided by GHCN-D is not always recorded regularly. Valid records are compared with simultaneous satellite-based observations. Records based on PSMOP-Namco provide various variables (SD, Ta and Ts) in the comparison study.

2.4 SDs derived by reanalyses

To compare with ground measurements and high-resolution satellites, SDs from ERA5 and ERA5-Land are reassessed over the TP. Comparison focuses on the period 2017–2020 when the in situ and remote sensing observations are relatively abundant. ERA5, as the 5th generation of reanalysis from ECMWF, supersedes previous ERA-Interim data (Hersbach et al. 2020). Previous studies have shown that improvements in ERA5 include a better representation of

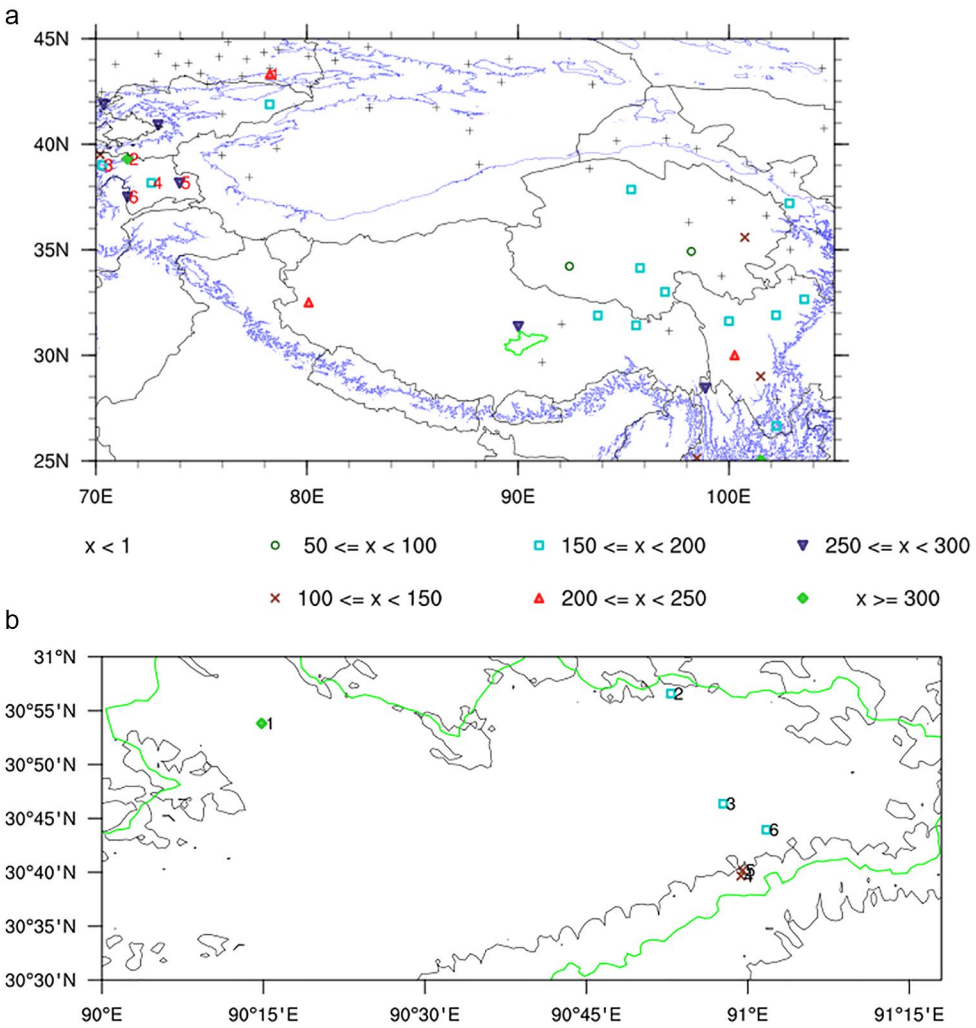

Fig. 2 (a) The location of GHCN-D stations with snow depth observations during 2016–2020. Marks correspond to numbers of sampling of Sentinel-1 snow depth retrievals for the period 2017 through March 2020. Representive sites in the west of TP (marked as 1–6) are investigated evolutions of SDs later. The Namco watershed is circled in green line. (b) 6 sites at Namco intensive observation experiment (PSMOP-Namco) during July 2019-June 2020

weather events, cloud cover extents, surface irradiance parameters, atmospheric water fluxes and other variables with respect to the former ERA-Interim dataset (Lei et al. 2020; Eicker et al. 2020; Yan et al. 2020; Zhao and Zhou 2019). The previous study suggested that overestimation in ERA5 is also due to lack of assimilation of IMS at high altitudes (Orsolini et al. 2019). As both SD and FSC are diagnostics based on the prognostic snow mass and density, and FSC as a function of SD, SD is investigated only in this study. Other variables like 2 m air temperature and the first level soil temperature (Ta and Ts) derived from ERA5 are also employed to correspond to in situ observations.

SD derived from the ERA-Land is achieved through global high resolution numerical integrations of ECMWF land surface model driven by the ERA5. The main advantage of ERA5-Land is its 9 km resolution compared to 31-km model resolution of ERA5. ERA5-Land SD presents a mixed performance in comparison to those of ERA5, depending on geographical location and altitude (Muñoz-Sabater et al. 2021).

In addition to ERA5 and ERA5-Land, SD and FSC derived from the NASA Modern-Era Retrospective analysis for Research and Applications Version 2 (MERRA-2) are also used in the comparison. Previous studies reported that MERRA-2 was in better agreement with in-situ observations than ERA5s (Orsolini et al. 2019; Reichle et al. 2017). MERRA-2 data during 2018–2020 is investigated at ground-based sites, together with ERA5s.

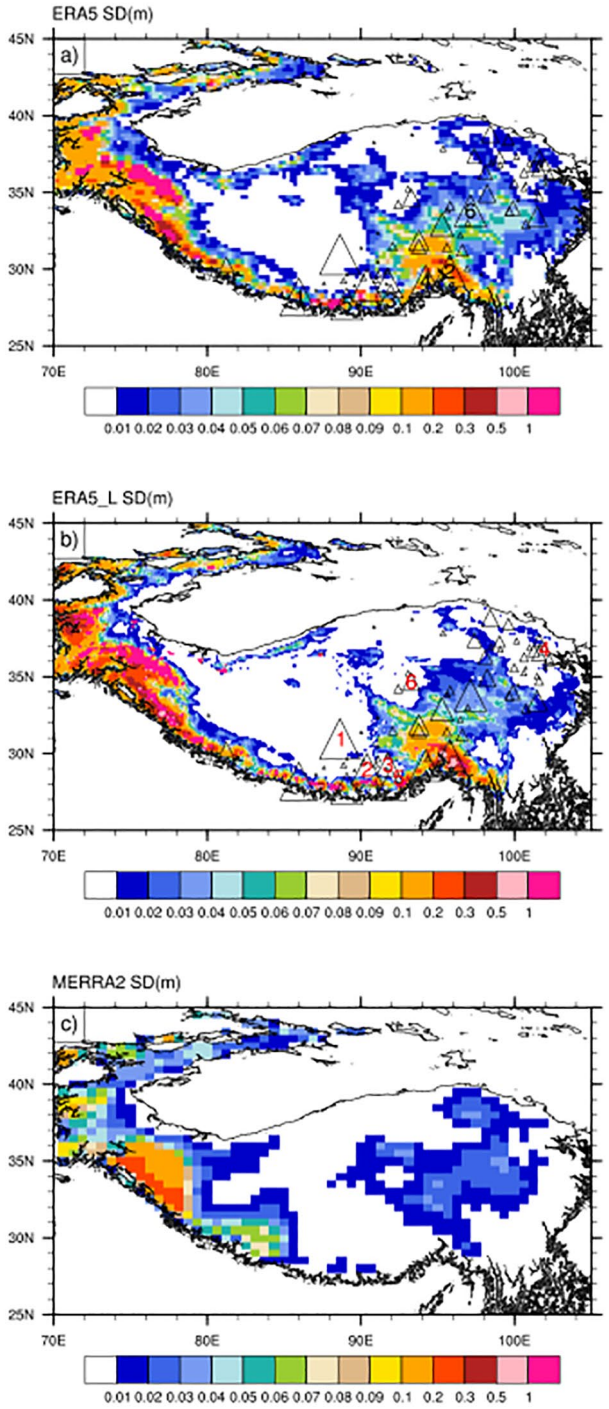

Fig. 3 Averaged SD (m) during September 2018 to August 2019 derived from ERA5 (a), ERA5-Land (b) and MERRA-2 (c). In situ observed precipitation at 91 stations is accumulated when correspondence snow cover presence is observed by MODIS (FSC > 10%), shown with triangles. Representive sites with more precipitation and larger SD (the largest 6 products of total precipitation and ERA5 SD) are shown (a,1–6 marked with black number), while 6 sites with more precipitation but relatively small SD (the largest 6 ratios of precipitation and ERA5 SD) are shown (b, 1–6 marked with red number)

2.5 Methods

Areal conservative remapping method is utilized to interpolate from high-to-low resolution grids, which can do a better job of preserving the value of the integral of data between the fine resolution source and destination grid than the conventional bilinear remapping method. Satellite-based FSC (500-m) is redistributed to 31-km resolution of ERA5. Independent datasets including FSC from MODIS and SDs from reanalyses, Sentinel-1 and in-situ observations are investigated to reveal snow states and changes over the TP. Similarity and difference are highlighted using the correlation coefficient and the root-mean-square-difference (RMSD). The statistical significant of a linear correlation coefficient is determined by the probability value (rtest). The Student's t-test is used to estimate the hypothesis that the population variances of a pair of samples (e.g., in-situ SD and ERA5 SD) are equal or different.

3 Results

3.1 Variability of snow cover and snow depth

Satellite-based FSC and SD highlight that snow states are rather heterogeneous across the TP (Fig. 1). Figure 3 presents averaged SD in the period September 2018-August 2019 derived from reanalyses (ERA5, ERA5-Land and MERRA-2). Spatial distributions of SDs from ERA5s are consistent with satellite-based SD. They highlight exceeding 10 cm SD over Tianshan, Pamir, Karakoram, Himalaya, Nyainqentanglha and Tanggula, but less than 1 cm over the interior TP. SD from ERA5-Land is even larger than that of ERA5 over mountainous regions in the west. Spatial distribution of SD from MERRA-2 shows different features between the west and east of TP. However, magnitudes are much lower than those of ERA5s over mountainous regions, particular glaciers. Comparison with Sentinel-1 and ERA5s, MERRA-2 underestimates SD over Nyainqentanglha and Tanggula. Differences imply effects of different land surface schemes in reanalyses.

In-situ observation of precipitation at 91 stations over TP in the period September 2018-August 2019 is analyzed as auxiliary data. Precipitation is treated as snowfall and accumulated when corresponding FSC from MODIS exceeds 10%. Amounts of snowfall range from 1 to 55 cm shown in Fig. 3. The hypothesis is that more observed snowfall corresponds to larger SDs from reanalyses, and vice versa. It is generally true as more precipitation occurs over mountainous regions and the less over the interior TP. Representive sites with more precipitation and larger SD (the largest 6 products of accumulated snowfall and ERA5 SD, 1–6

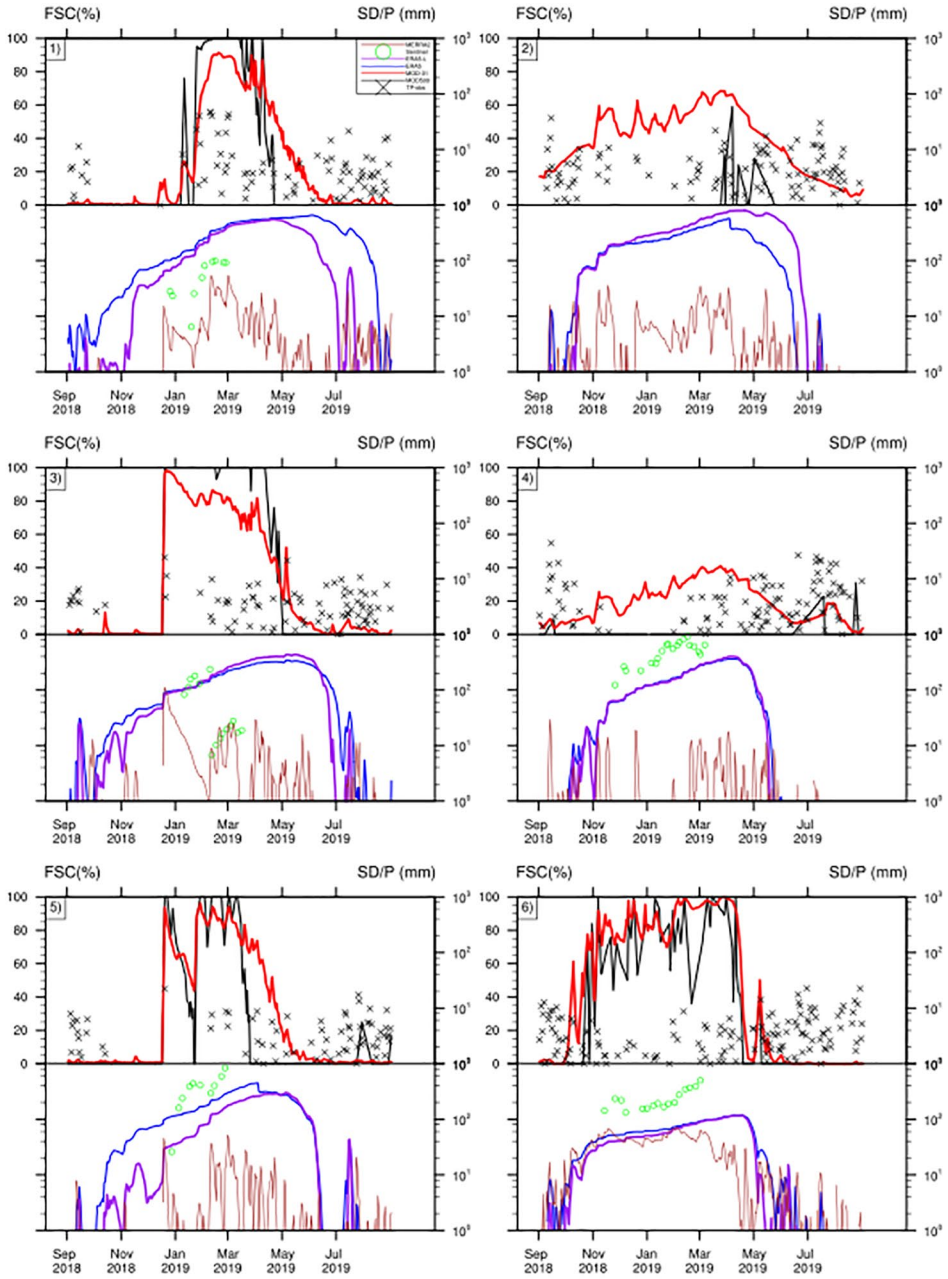

Fig. 4 FSC derived from MODIS (500 m resolution and regridded 31 km, black and red lines), in-situ precipitation (black cross), SD from Sentinel-1 (green circle), SD derived from ERA5, ERA5-Land and MERRA-2 (blue, purple and brown lines) at representive sites (Fig. 3a) in the period September 2018-August 2019

marked in Fig. 3a) are selected to display time series during one snow year in Fig. 4. On the other hand, reasons for the inconsistency of the hypothesis at a few stations of the interior TP are also explored in Fig. 5. At those 6 stations (the largest 6 ratios of snowfall and ERA5 SD, 1–6 marked in Fig. 3b), accumulation of snowfall is relatively large but SD is less than 1 cm on average.

Figure 4 displays FSC derived from MODIS (500 m resolution and regridded 31 km), in-situ precipitation and SDs from ERA5, ERA5-Land, MERRA-2 and Sentinel-1 in the period September 2018-August 2019 at representive 6 sites. Precipitation occurs frequently during the year due to mountainous regions. Precipitation is slightly less in winter, but observed precipitation in cold seasons is coherent with increases in FSC. Compared with fine-scale FSC, its coarse resolution shows continuous snow presence during winter and spring seasons. Effect of terrain complexity on different resolutions of FSC is obvious in mountainous regions.

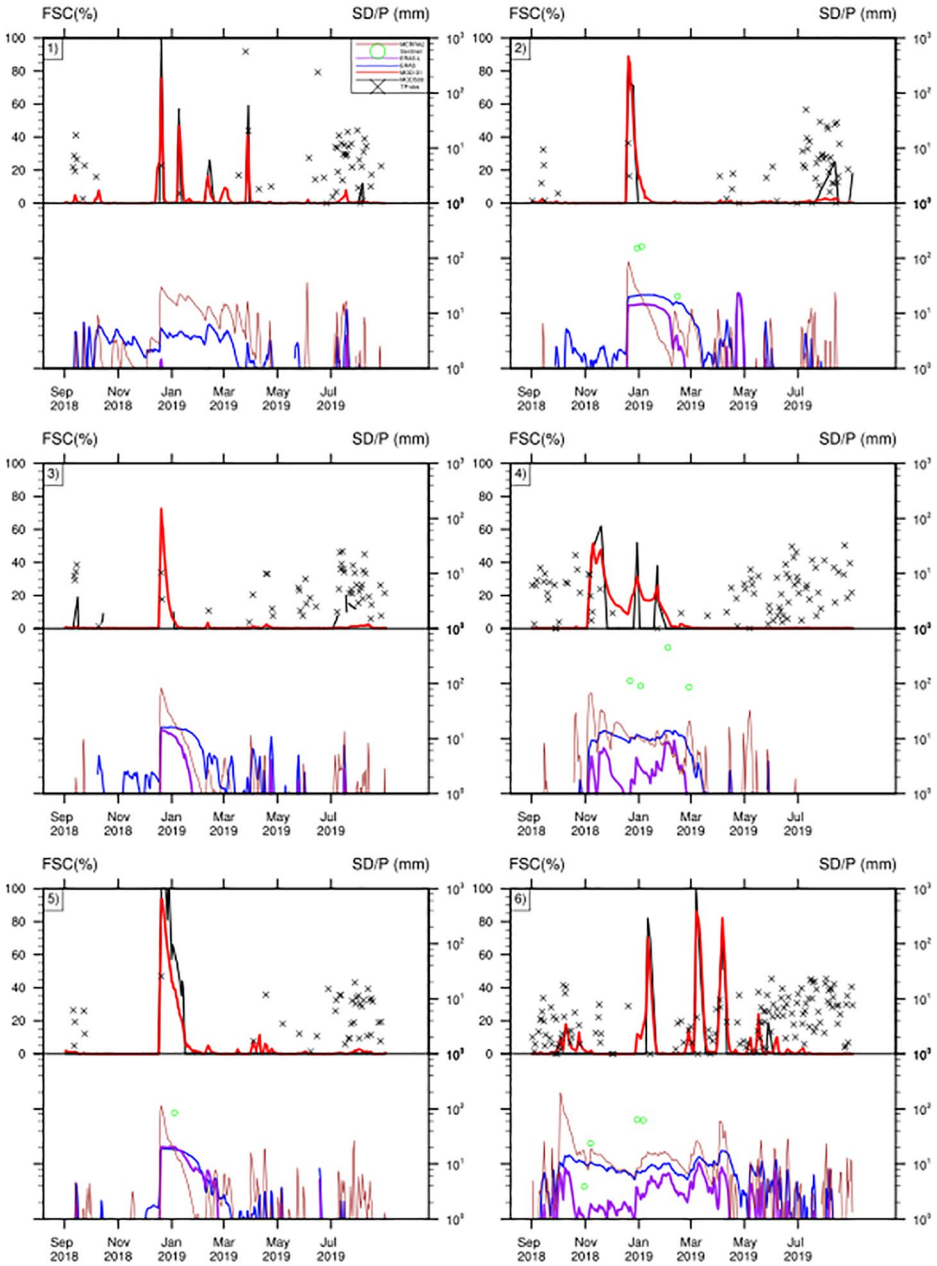

Fig. 5 Same as Fig. 4, but at representive 6 stations (Fig. 3b)

SDs from ERA5s are similar and remain above the average of 10 cm at representive sites in the snow season, while satellite-based SDs have comparable magnitudes. Maximums of SDs from ERA5s and Sentinel-1 can reach tens of centimeters. Magnitudes of SDs from MERRA-2 are smaller than other datasets because MERRA-2 underestimates SD and FSC in the southern edge of TP (Fig. 3c). Only at the 6th site, MERRA-2 SD is comparable with others in magnitudes (~ 10 cm) and temporal variations. Compared with rapid decreases in FSC during spring and early summer, delayed ablation in ERA5s implies biases of overestimates of SDs.

Figure 5 shows precipitation, and FSCs and SDs at another 6 representive sites where accumulated snowfall (averaged SD) is relatively large (small) in the interior TP. Unlike stations in mountains, FSCs of fine and coarse resolutions both indicate snow presence and absence in the interior TP from time to time even during winter. Although observed precipitation is less frequent, satellite-based FSC indicates snow presence with occurrence of precipitation. Reanalyses SDs are less than 1 cm on average. SDs from

scattered observations of Sentinel-l can be ten times larger than reanalyses, which may be impacted by high sensitivity of Sentinel-1 to deep snow even at small spatial scale. SD derived from ERA5-Land is the smallest, and variation especially is consistent with that of FSC. SDs from MERRA-2 are slightly larger than those from ERA5s.

Figure 6 shows the monthly mean of MODIS FSC (500 m) over the TP during September-April in the period of 2017–2020. Annual cycle is distinct over most of the TP. In Karakoram and Kunlun mountains, there are glaciated and persistent snow cover regions. High values of FSC begin in September and correspond well with mountains, including Tianshan, Pamirs, Karakoram, Himalayas, Kunlun, Nyainqentanglha, Tangula and Hengduan. Maximum FSCs occur in March, consistent with spring precipitation observed in Figs. 4 and 5. FSCs exceed 90% in mountains, while it is less than 40% in the interior TP. There is snow-free or lower than 10% in the large area of the interior TP. Overall, the processes of expansions (September to the following March) and contraction (April to August) demonstrate temporal and spatial variations of FSCs.

Figure 7 illustrates monthly mean of Sentinel-1 SD (1 km) over the TP during September-April in the period of 2017–2020. Although insufficient samples over the TP on temporal and spatial resolutions have been found, the annual cycle of satellite-based SD displays the accumulation process from September to the following February. It is consistent with expansion of FSC. In general, SD and FSC are most abundant in the northwest that is directly exposed to the westerly jet stream. There is above 50 cm SD, while the highest values are more than 1 m among the mountain ranges. Another significant amount of peak SD is located in the southeast. SD is about 10–20 cm over the Tangula Shan. SD can reach more than 1 m at the Nyainqentanglha mountain ranges. Shallow and patch snow is dominant in the interior TP where SD is about 1 cm.

Satellite-based SD from Sentinel-1 starts to melt in March, but FSC from MODIS maintains the largest of a year. SDs significantly reduce over the Hengduan and Tangula Shan. It may be related to spring snowfall that can extend snow cover but cannot maintain SD. It may also be related to the reduced volume scattering of the wet snow that results in an underestimation of SD (Lievens et al. 2019). Shallow snowpack in the interior TP begins to melt out in February. Snowpack continues to melt-out through March. Apart from glaciers, most of areas are snow-free or less than 5 cm after April.

Figure 8 displays the annual cycle of SD derived from ERA5 and ERA5-Land during four months (October, December, Febuary and April) in the period 2017 to 2020. There are great similarities between ERA5 and ERA5-land. Both ERA5 and ERA5-Land SDs present snow accumulation processes over mountainous regions, comparable with satellites. SD from ERA5-Land is relatively large (small) over mountainous regions (the interior of TP) compared with ERA5 (shown in Fig. 8). Differences imply effects of dynamical downscaling (of ERA5) and corrected thermodynamic input. Nevertheless, overestimates of reanalyses SDs over mountains during April are significant compared with satellite-based SD.

3.2 Matters of scale

Based on samples of GHCN-D (Fig. 2a) and PSMOP-Namco (Fig. 2b), histograms of SDs are compared among different datasets in Fig. 9. In-situ observations, Sentinel-1, ERA5 and ERA5-Land are simultaneously sampled during 2017–2020. 608 samples are compared in total. Values are sorted in range of bins (< 0.01 m, 0.01–0.05 m, 0.05–0.1 m, 0.1–0.2 m, 0.2–0.3 m, 0.3–0.4 m, 0.4–0.5 m, 0.5-1 m, and > 1 m). From snow-free (< 1 cm) to deep snow categories, samples of ground measurements decrease gradually. It reflects the effect of relatively low altitudes of ground stations. Compared with in-situ observations, Sentinel-1 has larger portions of snow absence (46%) and deep snow (above 50 cm, about 20%) categories. Because Sentinel-1is less sensitive to thin snow, there are few samples with 1–10 cm. Simulated SDs in ERA5 and ERA5-Land are generally comparable with in-situ observations. There are slightly more deep snow samples in SD of ERA5-Land, while more snow free or thin snow samples (less than 5 cm) in ERA5. Different features of sample distributions between ERA5 and ERA5-Land are likely attributed to spatial resolutions.

Figure 10 compares SDs (excluding snow-free conditions) of in-situ measurements with ERA5-Land, ERA5, MERRA-2 and Sentinel-1. Because there are 397 samples, correlations between ground-based measurements and gridded datasets (ranging from 0.3 to 0.47) are all significant based on the t-statistic test. The RMSD indicates that SD of ERA5-Land (0.14) can fit better with in-situ observations over the TP. Furthermore evaluations based on the Student's t-test (t-value being 1.46) provide that the sample means only from ERA5-Land and in-situ are from the same population. The sample means of ERA5 and MERRA-2 are statistically independent from in-situ observations (t-value being 7.64 and 7.82). Underestimates of ERA5 and MERRA-2 are clear. RMSDs are 0.15. Overestimate of satellite-based SD is distinct with RMSD being 0.37.

The ERA5-Land skill is somewhat greater than that of ERA5 and MERRA-2 in terms of comparison with in-situ observations of SD. The conclusion is different from previous studies, which may be attributed to selected samples. Samples from the western mountains with deep snowpack in

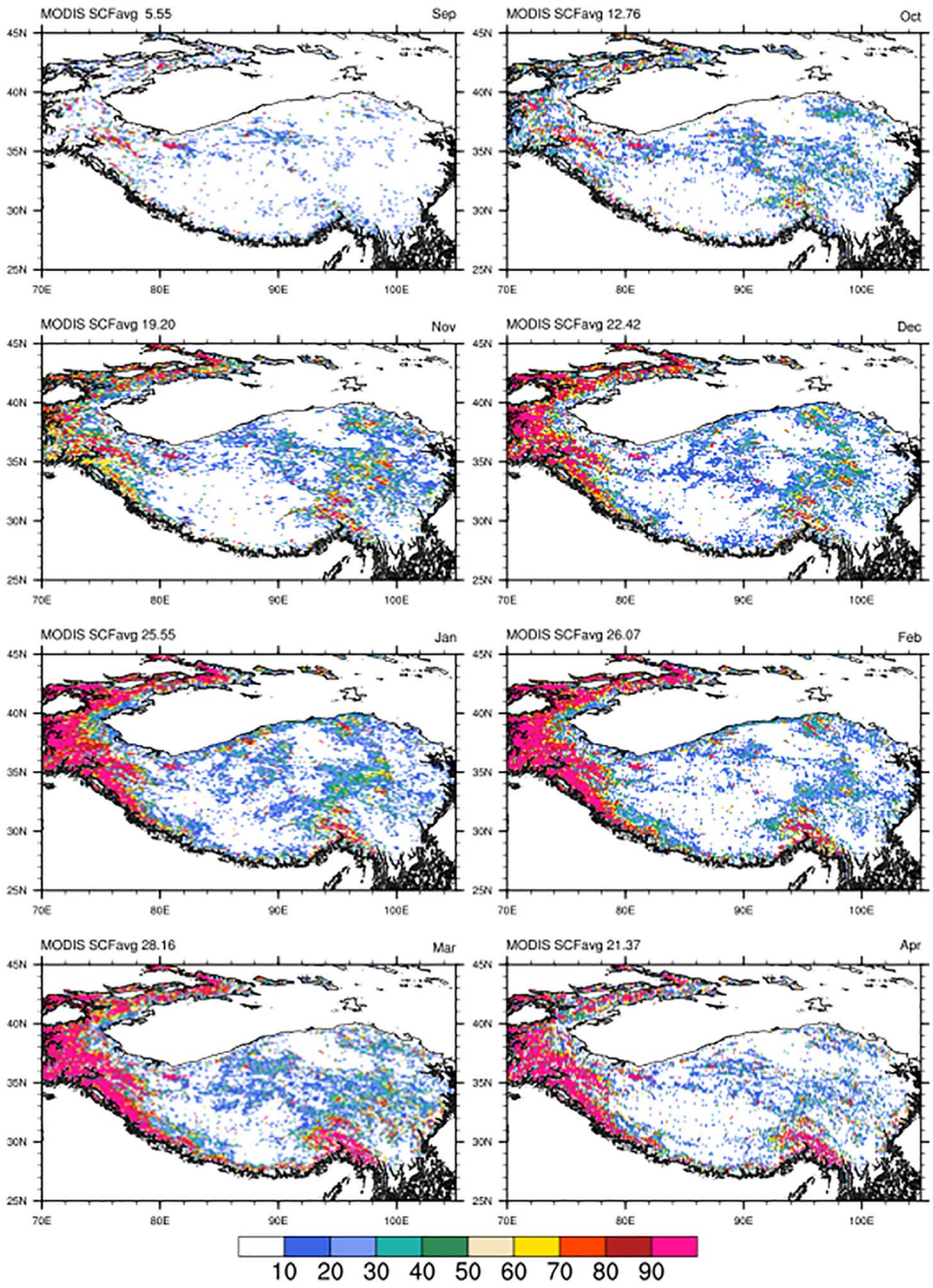

Fig. 6 Monthly mean of FSC (MODIS 500 m) over the TP from September to April in the period of 2017–2020

this work are not investigated by previous studies. Figure 11 presents comparison of SDs from ground-based observations with reanalyses (ERA5-Land, ERA5 and MERRA-2) and satellite measurements at 6 sites of the western TP (marked in Fig. 2a) during September 2018-June 2020. FSCs derived from MODIS agree well with times when the sites are snow covered in the in-situ measurements or reanalyses. Coherent with fine scale variations of FSCs, ground-based SDs is most dynamic particularly early in the snow season and at the end. Large SDs (tens of centimeters) can accumulate and last only late in the snow season (January-March). SD derived from Sentinel-1 has comparable magnitudes with in-situ observations. Underestimates SDs particularly for deep snow are found in reanalyses. ERA5-Land is slightly larger than ERA5 and MERRA-2. It is worth to note that SD from MERRA-2 has been modified by FSC which is shown together with MODIS. The benefit includes that times of the start and end of snowpack in MERRA-2 are consistent with in-situ observations.

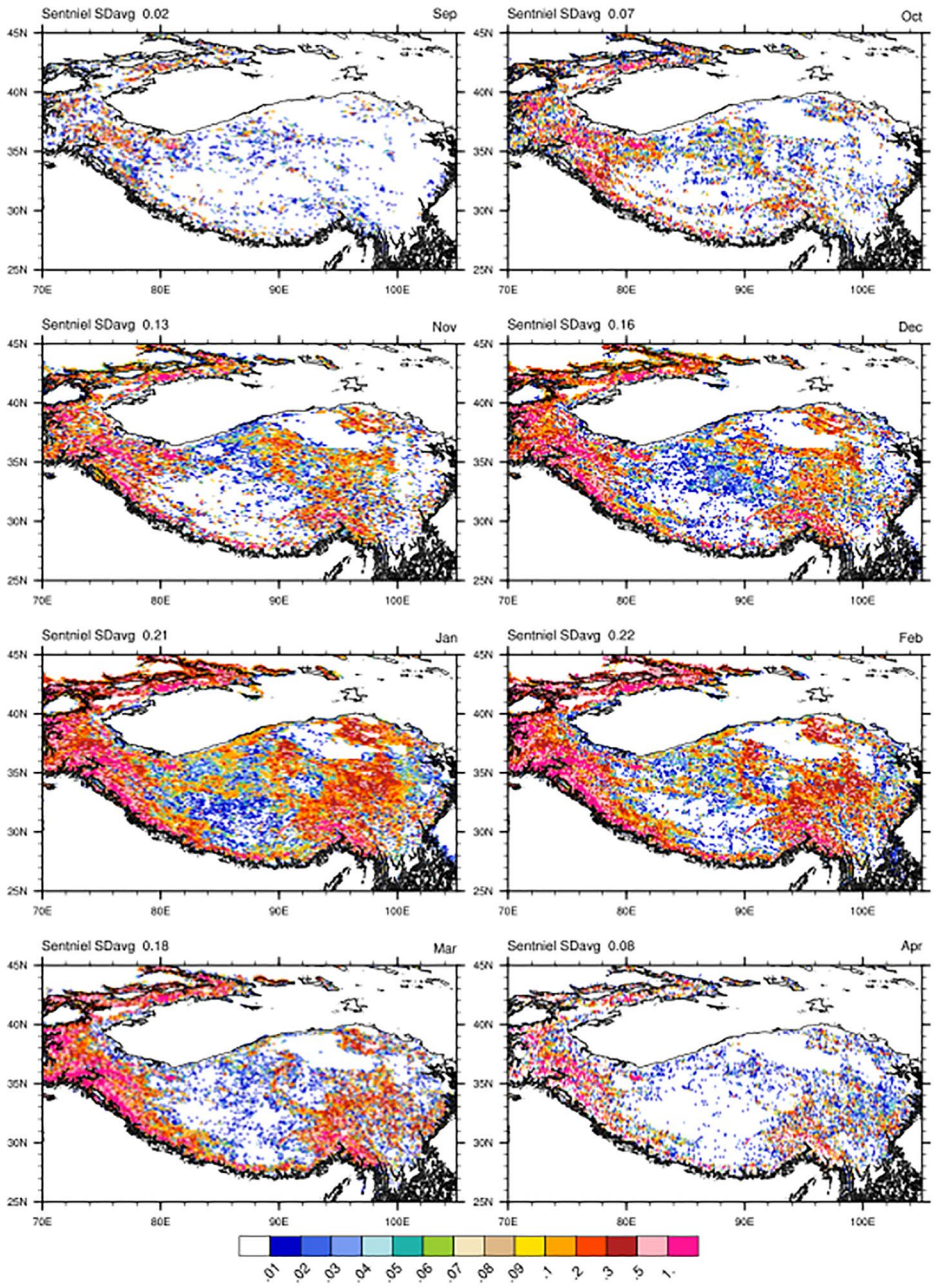

Fig. 7 Monthly SD derived by Sentinel (1 km) over the TP from September to April in the period of 2017–2020

Based on the intensive observational experiment during July 2019-June 2020 at 6 stations of the Namco watershed, Fig. 12 displays in-situ SDs, SDs derived from Sentinel-1, ERA5-Land, ERA5 and MERRA-2. FSC monitored by MODIS is also investigated at 500 m and 31 km resolutions. The first two sites locate in the north and west of Namco Lake (Fig. 2b). Sporadic snow or snow-free conditions are dominant based on ground measurements. Short-lived snowpack is characterized by satellite-based FSC, consistent with in-situ observations. SD of ERA5-Land represents snow absence well (less than 1 cm). ERA5 shows transient snowpack in the first site, but it suggests constant thin snowpack during the snow season in the east site. Frequent occurrences of FSC (above 10%) from MODIS imply the existence of snow in the 31-km grid.

At four sites located in the south and east of Namco Lake, SDs over 10 cm and more are observed on the ground. Stable snowpack lasts a few months from November to February. Different evolution features are notable at four sites, which are related to locations and altitudes. In general,

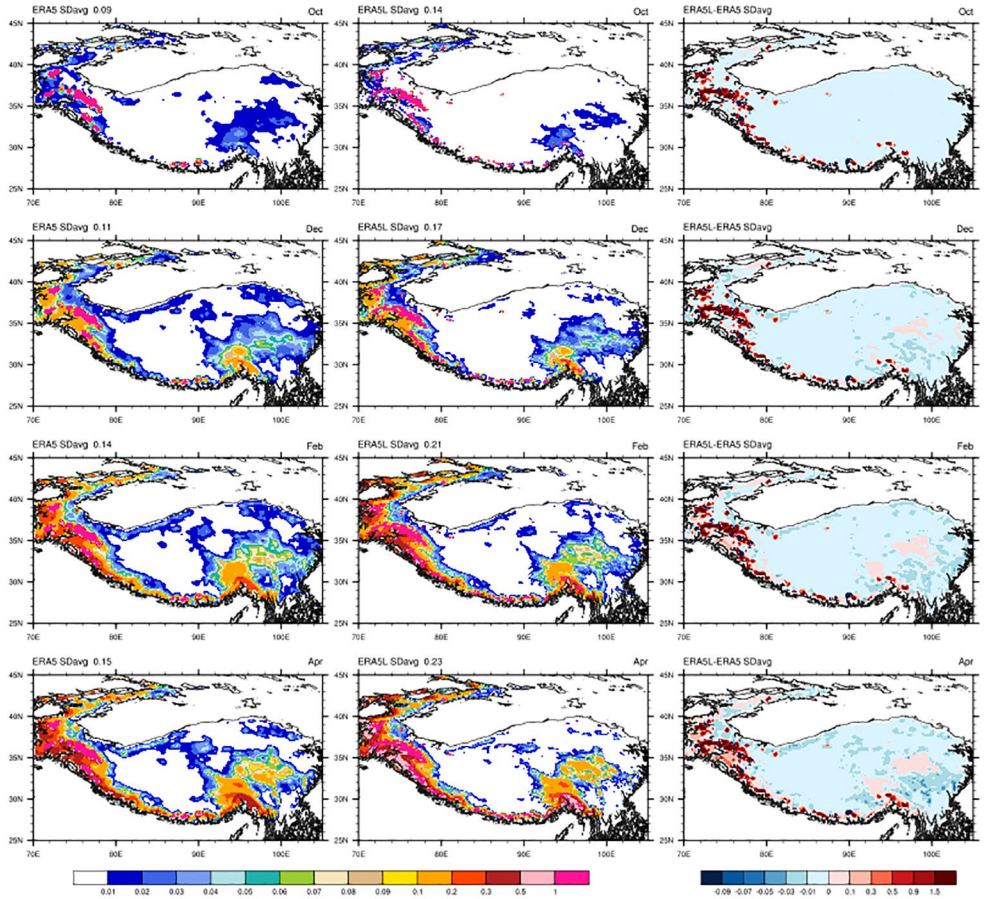

Fig. 8 Monthly SDs from ERA5 and ERA5-Land in October, December, February and April during 2017–2020, together with differences between ERA5-Land and ERA5 over the TP

ground measurements represent relatively slow process of decreases after SDs rapidly reach a peak. It responds to snow compaction or sublimation processes. Snowpack melts out during late March.

Satellite-based SDs and FSC match the start and end of deep snowpack well. FSC derived from MODIS reasonably describes daily and monthly variations of snowpack. MODIS FSC (500 m) indicates snow presence at sites with a relatively high altitude during October and April-June. MODIS FSC of 31 km resolution ranging from 10 to 40% during transition seasons corresponds to patchy snow features. It should be noted that the grid of 31 km resolution (same with ERA5) covers these four sites. Sentinel-1 SD retrievals are always larger than in-situ measurements and reanalyses.

Four sites correspond to two grids of 9 km resolution of ERA5-Land, which shows interesting differences related to altitudes. ERA5-Land is larger than ERA5 and closer to in-situ measurements especially at the site with relatively high altitude. Effect of terrain complexity on snow states can partly explain the difference between in-situ observations and gridded SD.

SDs of ERA5 and MERRA-2 represent a mean snow state of those sites with about 1 cm due to coarse resolutions. Overestimates at first two sites in the north and west of Namco Lake are obvious, while underestimates are distinct at other four sites located in the south and east. FSC from MERRA-2 shows very little snow cover during the year, which is inconsistent with FSC from MODIS.

Delayed ablation of snowpack in ERA5s during April and May is distinguished. It could imply errors in simulating snow melting process in reanalysis. It could also be attributed to wrongly classified rainfall to snowfall during spring and early summer seasons (Fig. 4).

Figure 13 shows comparison of temperatures (Ta and Ts) that were recorded in PSMOP-Namco intensive experiment during July 2019-June 2020. Corresponding Ta and Ts derived from ERA5 are also illustrated. Annual cycle of temperatures is similar between ERA5 and in-situ observations. Differences of temperatures between ERA5 and in-situ observations highlight relatively biases during spring. In

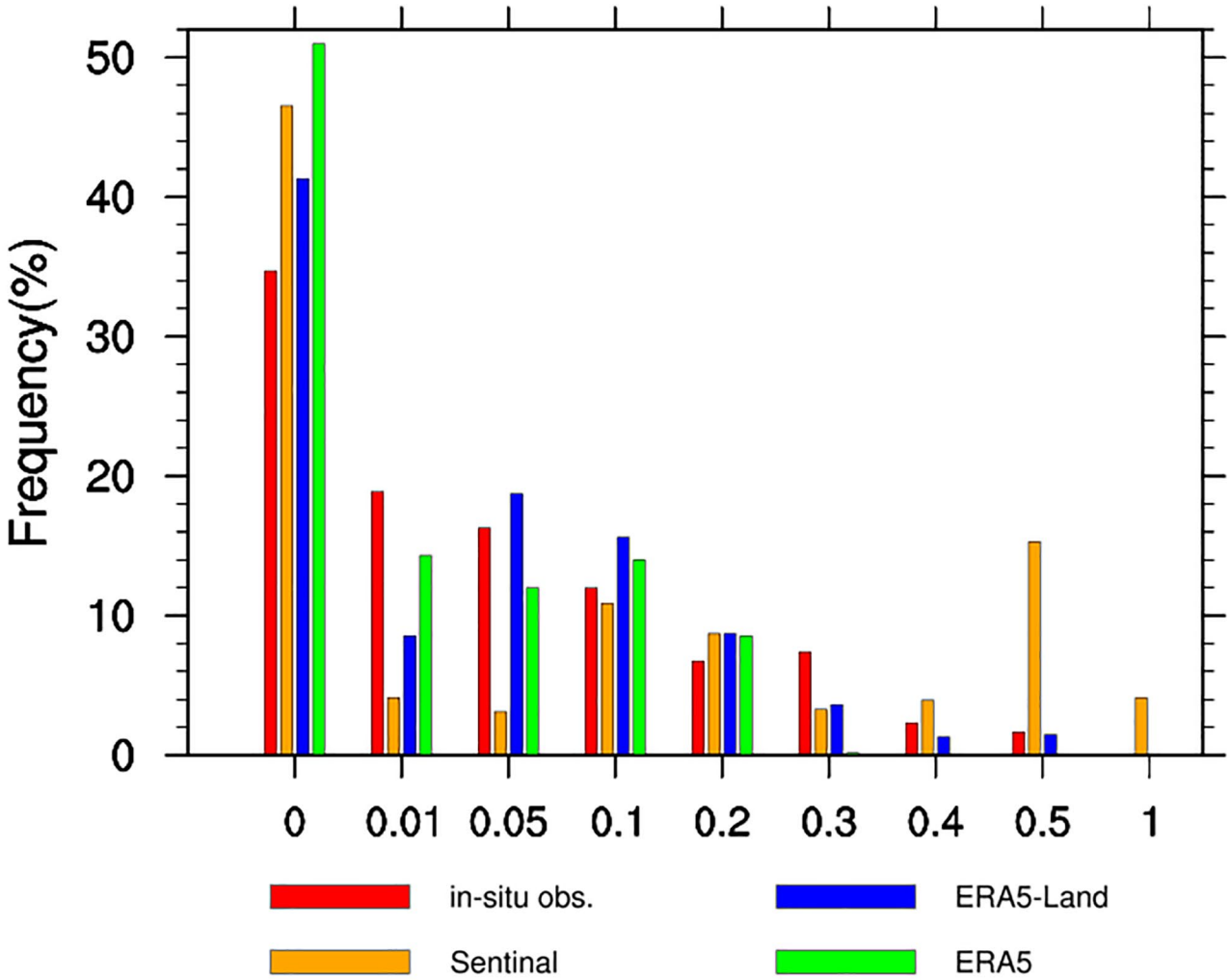

Fig. 9 Histograms show SD (simultaneously sampled in GHCN-D and PSMOP-Namco, Sentinel-1, ERA5 and ERA5-Land) fall in range of bins (< 0.01 m, 0.01–0.05 m, 0.05–0.1 m, 0.1–0.2 m, 0.2–0.3 m, 0.3–0.4 m, 0.4–0.5 m, 0.5–1 m, and > 1 m)

snow-free condition, biases are small and coherent between Ta and Ts (Figs. 12 – 1). With occurrence of deep snow, ERA5 tends to have cold (warm) biases of Ta (Ts) during winter compared with in-situ observations. However, warm biases of Ts turn to cold biases during spring and early summer seasons. The reason is that observed Ts increase rapidly due to snow absence. Errors of ablation process in ERA5s during spring and early summer hinder increase in Ts.

4 Discussion and conclusions

The lack of observations is the biggest challenge on the TP. A strategy that combines sets of station observations and remote sensing measurements and model simulations is of great importance to improve understanding the cryosphere and its interaction with climate (Yao et al. 2019). The extent and variability of the snowpack over the TP are vital because of roles in the surface energy balance and in the hydrological cycle (You et al. 2020). Radiative and thermodynamical feedbacks of snow potentially impact on weather and climate system at the local and surrounding areas through its land-atmosphere interaction (Xue et al. 2017; Liu et al. 2020).

The seasonal snow cover over the TP is distinguished because of its distinctive shallow, patchy and short-lived snowpack (Orsolini et al. 2019). 500-m MODIS FSC shows that snow cover is unevenly distributed (Fig. 1b). Apart from the highest mountains, FSC can be up to about 40% in the eastern part, and it is less than 10% over the interior TP (Fig. 6). The lack of fully covered snow at spatial and

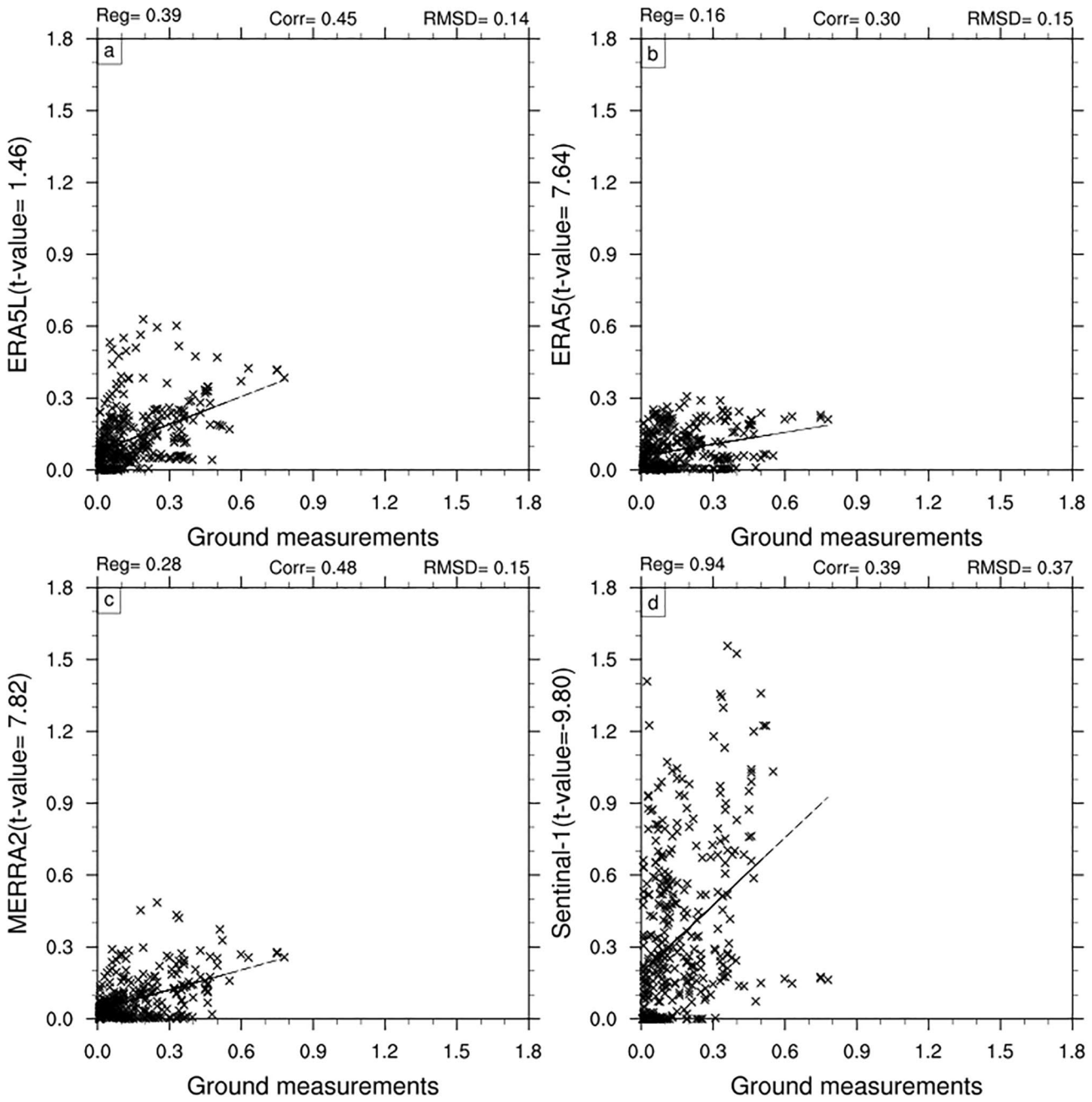

Fig. 10 Comparisons of SD in ERA5-Land, ERA5, MERRA-2 and Sentinel-1 retrievals (1-km) with in-situ observations of GHCN-D and PSMOP-Namco (excluding snow–free samples) by scattered points and regressions. Correlation coefficients are 0.45, 0.30, 0.48 and 0.39, respectively. RMSDs range from 0.14, 0.15, 0.15 to 0.37

temporal scales is a dominant feature over the large area of TP throughout cold seasons (Pu and Xu 2009).

MODIS FSC and in-situ observations are reasonable connected (Figs. 4, 5, 11 and 12). SDs with thin snow (1–5 cm) correspond a wide range of FSC from 0 to above 90%. Considering different scales of two datasets, fine-scale variations at both temporal and spatial domains are crucial to understand the complicated snow effects on weather and climate over the TP. Wide range of FSC indicates terrain complexity and its impacts on snow states and changes.

The spatial distribution and seasonal variation of SD derived from Sentinel-1 (Figs. 1d, 7, 11 and 12) are reasonably presented, especially for deep snow accumulation processes over mountainous regions during cold seasons. Sentinel-1 has difficulty in distinguishing thin snow from snow-free conditions because the penetration ability of

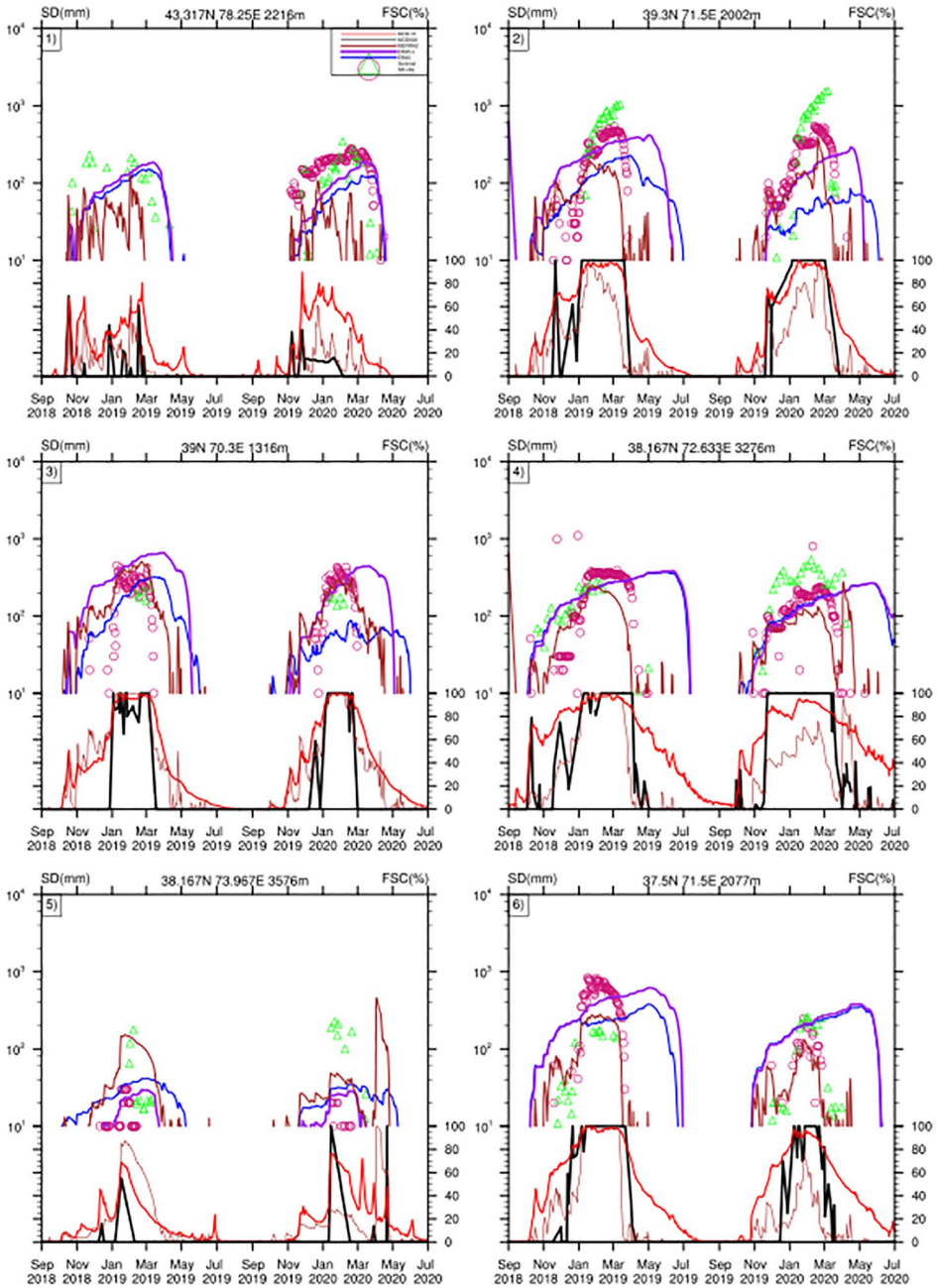

Fig. 11 SDs derived from ground measurements (dark pink circle), Sentinel-1 (green triangle), ERA5-Land (purple line), ERA5 (blue line) and MERRA-2 (brown line) at 6 sites of the west TP (marked in Fig. 2a) during September 2018-June 2020 are shown in the top. FSCs from MODIS (black line for 500 m vs. red line for 31 km) are also displayed in the bottom, together with FSC from MERRA-2 (brown line)

C-band microwave (Lievens et al. 2019). Limited valid retrievals of Sentinel-1 SD also hinder the systematic comparison. Nevertheless, Sentinel-1 SD provides valuable information for deep snowpack over the TP.

SD of reanalyses (ERA5 and ERA5-Land, shown in Fig. 8) well present snow accumulation processes during cold seasons. It is notable that reanalyses overestimate SDs during the ablation period (March-May) especially for deep snowpack (Figs. 4, 11 and 12). As the surface boundary condition of the atmosphere, delayed ablation can cause continuous unreal low temperature at surface and further impact seasonal evolution surrounding areas (Hong and Seol 2009; Duan et al. 2018; Liu et al. 2019; Li et al. 2020; Wang et al. 2020b; Orsolini et al. 2019). Comparison of temperatures (Fig. 13) between ERA5 and in-situ observations suggests the delayed ablation slows down the increase of Ts of ERA5

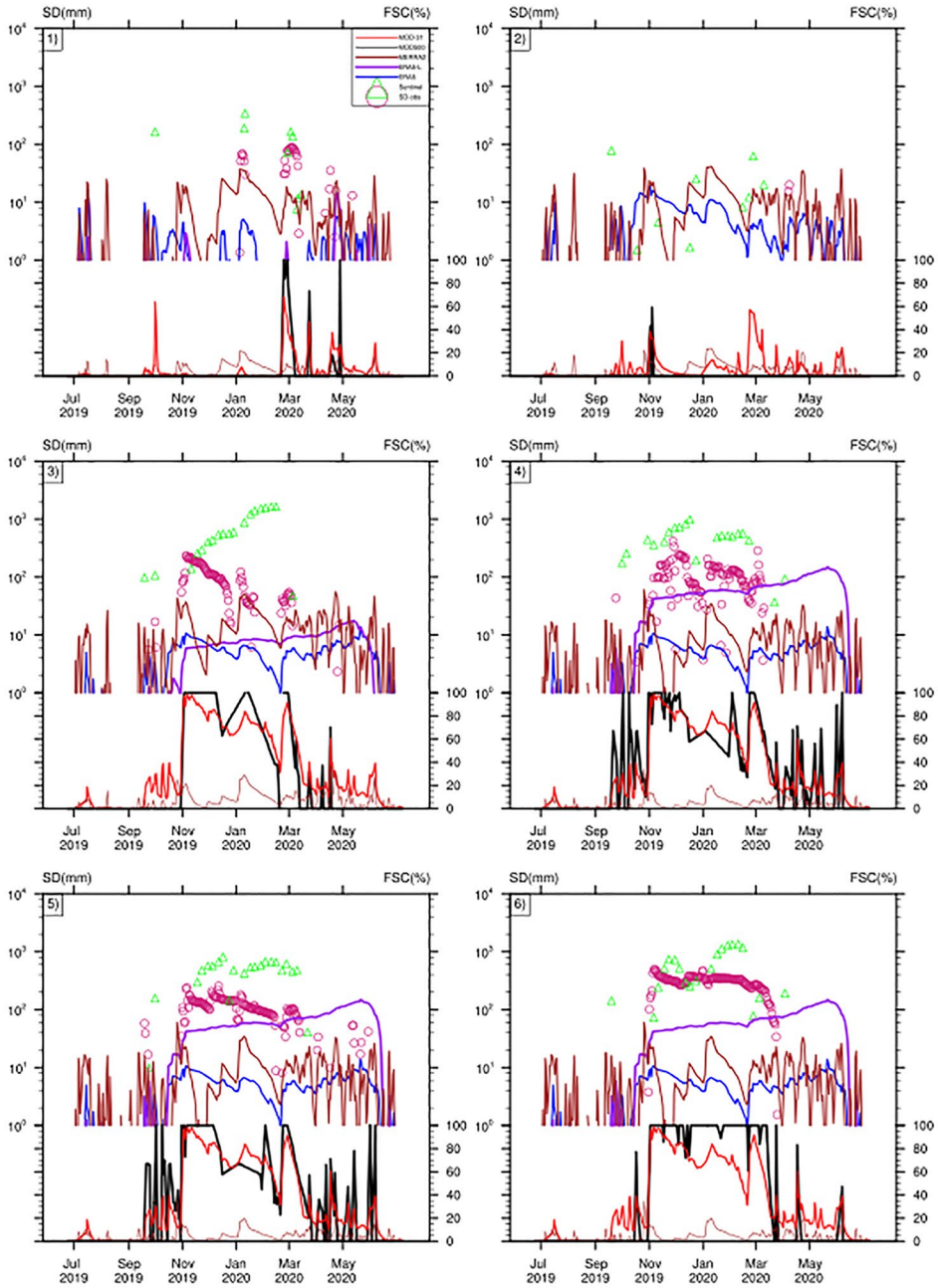

Fig. 12 Same as Fig. 11, but at 6 sites of Namco observational experiment (PSMOP-Namco, marked in Fig. 2b) during July 2019-June 2020

during spring and early summer, and further contributes cold biases about 4–8 °C. Biases in ERA5s' SD may impact on the land-atmosphere interaction and monsoon activity, which require further studies.

Compared with MERRA-2 data, ERA5s represent better spatial distributions of snowpack over the TP (Fig. 3). SD of MERRA-2 underestimates (overestimates) the deep (thin) snowpack (Figs. 4, 5, 11 and 12). Because SD of MERRA-2 is modified by FSC, temporal variations are consistent with in-situ observations. Reasonable annual cycle of Sentinel-1 SD (Figs. 4 and 7) is also attributed by auxiliary input data from IMS into the data retrieval algorithm (Lievens et al. 2019). Therefore, the way to further improve SD of ERA5 and ERA5-Land is in all likelihood to assimilate high-resolution datasets. It is important to introduce the heterogeneity over the TP (Bian et al. 2019; Orsolini et al. 2019; Yan et al. 2022).

This paper demonstrated matters of scale that may partly cause the discrepancy of snow states and changes among in-situ, remote sensing and reanalyses datasets. Previous

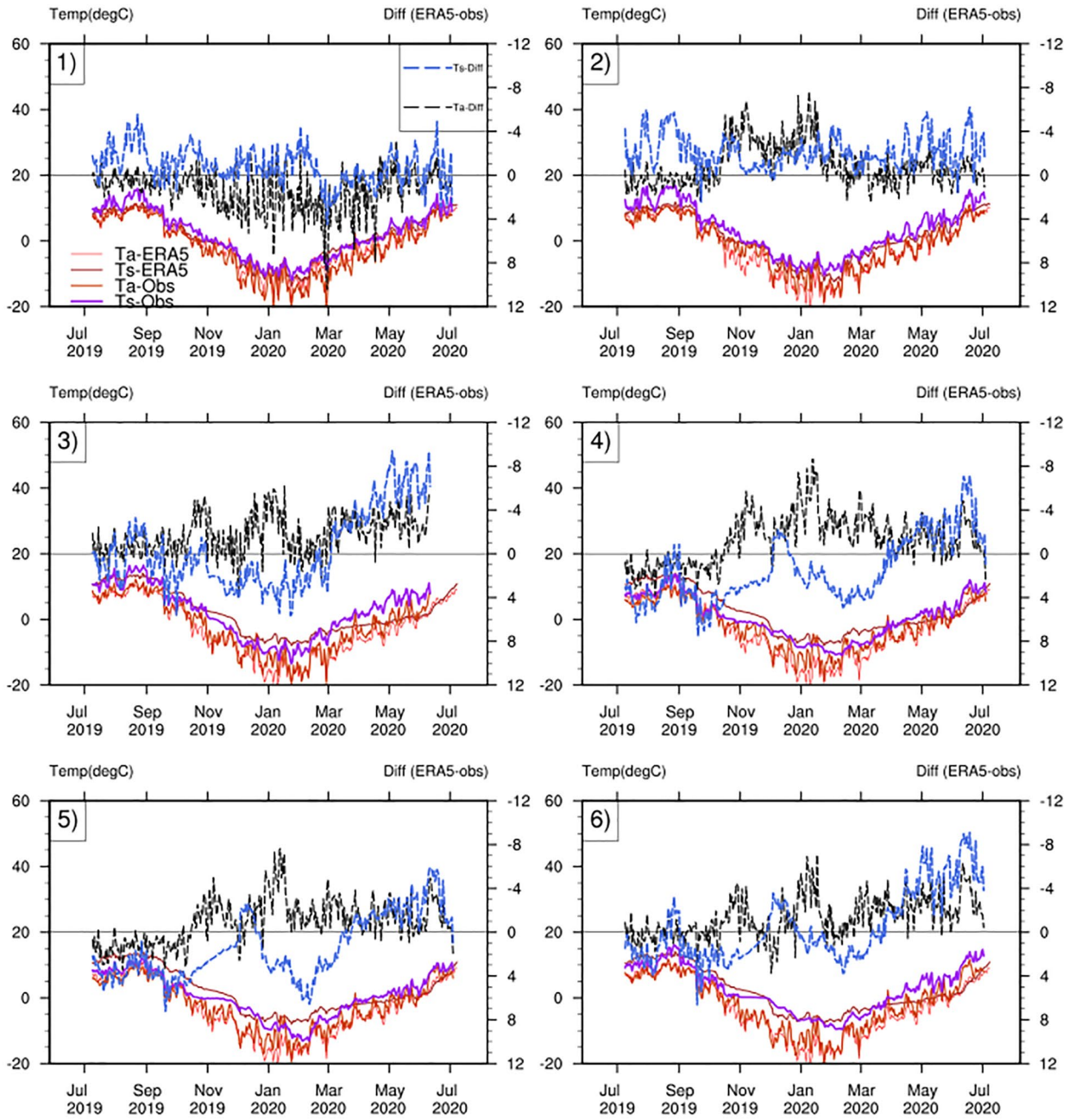

Fig. 13 Ta (dark red line) and Ts (purple line) derived from ground measurements in PSMOP-Namco intensive experiment and corresponding Ta (pink line) and Ts (brown line) derived from ERA5 are shown during July 2019-June 2020. Differences of Ta (black dashed line) and Ts (blue dashed line) between ERA5 and in situ are displayed

studies highlighted systematic model-based precipitation biases that might be the primary factor for the large overestimation of ERA5 SD (Orsolini et al. 2019; Muñoz-Sabater et al. 2021). Comparisons of in-situ SD observations provided by GHCN-D and PSMOP-Namco, MODIS FSC, SD of Sentinel-1, ERA5-Land, ERA5 and MERRA-2 indicate that fine resolution reanalysis dataset has better consistency to in-situ measurements. ERA5-Land matches in-situ observations better than ERA5 over the TP. Overestimates of ERA5s' SD are likely for shallow snowpack, but underestimates are found for deep snowpack particularly late in the snow season (Figs. 11 and 12). Improvements are displayed in ERA5-Land. A notable defect of ERA5s' SD is related to delayed ablation of deep snowpack during March-May. It causes cold temperature biases on the surface that may impact on the land-atmosphere interaction.

Acknowledgements This study was jointly supported by the National Key Basic Research Program of China (2018YFA0605400) and National Natural Science Foundation of China (Grant No. 42071408). We are grateful to Prof. Kun Yang for constructive discussions. We would like to thank anonymous reviewers.

Funding This study was jointly supported by the National Key Basic Research Program of China (2018YFA0605400) and National Natural Science Foundation of China (Grant No. 42071408).

Data Availability ERA5 and ERA5-Land are available through the C3S CDS Application Program Interface (API). The Sentinel-1 snow depth retrievals are available online at https://ees.kuleuven.be/ project/c-snow. Other datasets used and/or analyzed during the current study are available from the corresponding author on reasonable request.

Code Availability The source code is available from the corresponding author upon reasonable request.

Declarations

Conflict of interest To our knowledge there is no conflicts of interest of the material presented this work.

References

Basang D, Barthel K, Olseth J (2017) Satellite and Ground Observations of Snow Cover in Tibet during 2001–2015.Remote Sensing,9

Bian Q, Xu Z, Zhao L, Zhang Y-F, Zheng H, Shi C, Zhang S, Xie C, Yang Z-L (2019) Evaluation and Intercomparison of Multiple Snow Water Equivalent Products over the Tibetan Plateau. J Hydrometeorol 20:2043–2055

Bian Q, Xu Z, Zheng H, Li K, Liang J, Fei W, Shi C, Zhang S, Yang ZL (2020) Multiscale Changes in Snow Over the Tibetan Plateau During 1980–2018 Represented by Reanalysis Data Sets and Satellite Observations.Journal of Geophysical Research: Atmospheres,125

Bormann KJ, Brown RD, Derksen C, Painter TH (2018) Estimating snow-cover trends from space. Nat Clim Change 8:924–928

Cohen J (1994) Snow cover and climate. Weather 49:150–156

Dai L, Che T, Xie H, Wu X (2018) Estimation of Snow Depth over the Qinghai-Tibetan Plateau Based on AMSR-E and MODIS Data. Remote Sensing,10

Dozier J, Bair EH, Davis RE (2016) Estimating the spatial distribution of snow water equivalent in the world's mountains. WIREs Water 3:461–474

Duan A, Wu G, Zhang Q, Liu Y (2006) New proofs of the recent climate warming over the Tibetan Plateau as a result of the increasing greenhouse gases emissions. Chin Sci Bull 51:1396–1400

Duan A, Xiao Z (2015) Does the climate warming hiatus exist over the Tibetan Plateau? Sci Rep 5:13711

Duan A, Xiao Z, Wang Z (2018) Impacts of the Tibetan Plateau winter/spring snow depth and surface heat source on Asian summer monsoon: A review [J]. Chin J Atmospheric Sci (in Chinese) 755–766. doi:https://doi.org/10.3878/j.issn.1006-9895.1801.17247

Eicker A, Jensen L, Wöhnke V, Dobslaw H, Kvas A, Mayer-Gürr T, Dill R (2020) Daily GRACE satellite data evaluate short-term hydro-meteorological fluxes from global atmospheric reanalyses. Sci Rep 10:4504. https://doi.org/10.1038/s41598-020-61166-0

Frauenfeld OW, Zhang T, Serreze MC (2005) Climate change and variability using European Centre for Medium-Range Weather Forecasts reanalysis (ERA-40) temperatures on the Tibetan Plateau.Journal of Geophysical Research,110

Hall DK, Riggs GA, Salomonson VV, DiGirolamo NE, Bayr KJ (2002) MODIS Snow-Cover Products. Remote Sens Environ 83:181–194

Hao S, Jiang L, Shi J, Wang G, Liu X (2019) Assessment of MODIS-Based Fractional Snow Cover Products Over the Tibetan Plateau. IEEE J Sel Top Appl Earth Observations Remote Sens 12:533–548

Hersbach H, Bell B, Berrisford P, Hirahara S, Horányi A, Muñoz-Sabater J, Nicolas J, Peubey C, Radu R, Schepers D, Simmons A, Soci C, Abdalla S, Abellan X, Balsamo G, Bechtold P, Biavati G, Bidlot J, Bonavita M, De Chiara G, Dahlgren P, Dee D, Diamantakis M, Dragani R, Flemming J, Forbes R, Fuentes M, Geer A, Haimberger L, Healy S, Janisková RJ, Keeley S, Laloyaux P, Lopez P, Radnoti G, Rosnay Pd, Rozum I, Vamborg F (2020) S. Villaume & J.-N. Thépaut The ERA5 Global Reanalysis. *Quarterly Journal of the Royal Meteorological Society*, 146, 1999–2049

Hong S-Y, Seol K-H (2009) Relationship between the Tibetan Snow in Spring and the East Asian Summer Monsoon in 2003: A Global and Regional Modeling Study. J Clim 22:2095–2110

Jiang Y, Chen F, Gao Y, He C, Barlage M, Huang W (2020) Assessment of uncertainty sources in snow cover simulation in the Tibetan plateau. J Geophys Research: Atmos. 125, e2020JD032674 https://doi.org/10.1029/2020JD032674

Lei Y, Letu H, Shang H, Shi J (2020) Cloud cover over the Tibetan Plateau and eastern China: a comparison of ERA5 and ERA-Interim with satellite observations. Clim Dyn 54:2941–2957

Li W, Hu S, Hsu P, Guo W, Wei J (2020) Systematic bias of Tibetan Plateau snow cover in subseasonal-to-seasonal models. The Cryosphere 14:3565–3579. https://doi.org/10.5194/tc-14-3565-2020

Lievens H, Demuzere M, Marshall HP, Reichle RH, Brucker L, Brangers I, de Rosnay P, Dumont M, Girotto M, Immerzeel WW, Jonas T, Kim EJ, Koch I, Marty C, Saloranta T, Schober J, De Lannoy GJM (2019) Snow depth variability in the Northern Hemisphere mountains observed from space. Nat Commun 10:4629

Liu L, Ma Y, Menenti M, Zhang X, Ma W (2019) Evaluation of WRF Modeling in Relation to Different Land Surface Schemes and Initial and Boundary Conditions: A Snow Event Simulation Over the Tibetan Plateau. J Geophys Research: Atmos 124:209–226

Liu Y, Lu M, Yang H, Duan A, He B, Yang S (2020) Land–atmosphere–ocean coupling associated with the Tibetan Plateau and its climate impacts. REVIEW EARTH SCIENCES, & GuoxiongWu

Liu Y, Fang Y, Margulis SA (2021) Spatiotemporal distribution of seasonal snow water equivalent in High-Mountain Asia from an 18-year Landsat-MODIS era snow reanalysis dataset. *The Cryosphere*

Menne MJ, Durre I, Vose RS, Gleason BE, Houston TG (2012) An Overview of the Global Historical Climatology Network-Daily Database. J Atmos Ocean Technol 29:897–910

Muñoz-Sabater J, Dutra E, Agustí-Panareda A, Albergel C, Arduini G, Balsamo G, Boussetta S, Choulga M, Harrigan S, Hersbach H, Martens B, Miralles DG, Piles M, Rodríguez-Fernández NJ, Zsoter E, Buontempo C (2021) ERA5-Land: A state-of-the-art global reanalysis dataset for land applications. Earth Syst Sci Data. https://doi.org/10.5194/essd-2021-82. & J.-N. Thépaut

Orsolini Y, Wegmann M, Dutra E, Liu B, Balsamo G, Yang K, de Rosnay P, Zhu C, Wang W, Senan R, Arduini G (2019) Evaluation of snow depth and snow cover over the Tibetan Plateau in global reanalyses using in situ and satellite remote sensing observations. The Cryosphere 13:2221–2239

Painter TH, Berisford DF, Boardman JW, Bormann KJ, Deems JS, Gehrke F, Hedrick A, Joyce M, Laidlaw R, Marks D, Mattmann C, McGurk B, Ramirez P, Richardson M, Skiles SM, Seidel FC, Winstral A (2016) The Airborne Snow Observatory: Fusion of scanning lidar, imaging spectrometer, and physically-based modeling for mapping snow water equivalent and snow albedo. Remote Sens Environ 184:139–152

Pu Z, Xu L (2009) MODIS/Terra observed snow cover over the Tibet Plateau: distribution, variation and possible connection with the East Asian Summer Monsoon (EASM). Theoret Appl Climatol 97:265–278

Reichle RH, Draper CS, Liu Q, Girotto M, Mahanama SPP, Koster RD, De Lannoy GJM (2017) Assessment of MERRA-2 Land Surface Hydrology Estimates. J Clim 30:2937–2960

Shi J (2012) An automatic algorithm on estimating sub-pixel snow cover from MODIS. Quat Sci 32:6–15

Wang J, Huang X, Wang Y, Liang T (2020a) Retrieving Snow Depth Information From AMSR2 Data for Qinghai–Tibet Plateau. *IEEE JOURNAL OF SELECTED TOPICS IN APPLIED EARTH OBSERVATIONS AND REMOTE SENSING*, 13, 752–768

Wang W, Yang K, Zhao L, Zheng Z, Lu H, Mamtimin A, Ding B, Li X, Zhao L, Li H, Che T, Moore JC (2020b) Characterizing Surface Albedo of Shallow Fresh Snow and Its Importance for Snow Ablation on the Interior of the Tibetan Plateau. J Hydrometeorol 21:815–827

Wang X, Tolksdorf V, Otto M, Scherer (2020c) WRF-based dynamical downscaling of ERA5 reanalysis data for High Mountain Asia: Towards a new version of the High Asia Refined analysis. *International Journal of Climatology*

Wegmann M, Orsolini Y, Dutra E, Bulygina O, Sterin A, Brönnimann S (2017) Eurasian snow depth in long-term climate reanalyses. The Cryosphere 11:923–935

Wu G, Duan A, Liu Y, Mao J, Ren R, Bao Q, He B, Liu B, Hu W (2015) Tibetan Plateau climate dynamics: recent research progress and outlook. Natl Sci Rev 2:100–116. https://doi.org/10.1093/nsr/nwu045

Xu W, Ma L, Ma M, Zhang H, Yuan W (2017) Spatial-temporal variability of snow cover and depth in Qinghai-Tibetan Plateau. JOURNAL OF CLIMATE

Xue Y, Ma Y, Li Q (2017) Land–Climate Interaction Over the Tibetan Plateau. Oxford Research Encyclopedia of Climate Science

Yan H, Huang J, He Y, Liu Y, Wang T, Li J (2020) Atmospheric Water Vapor Budget and its Long-Term Trend over the Tibetan Plateau. Journal of Geophysical Research: Atmospheres

Yan D, Ma N, Zhang Y (2022) Development of a fine-resolution snow depth product based on the snow cover probability for the Tibetan Plateau: Validation and spatial–temporal analyses.Journal of Hydrology,604

Yao T, Xue Y, Chen D, Chen F, Thompson L, Cui P, Koike T, Lau WKM, Lettenmaier D, Mosbrugger V, Zhang R, Xu B, Dozier J, Gillespie T, Gu Y, Kang S, Piao S, Sugimoto S, Ueno K, Wang L, Wang W, Zhang F, Sheng Y, Guo W, Ailikun X, Yang Y, Ma SSP, Shen Z, Su F, Chen S, Liang Y, Liu VP, Singh K, Yang D, Yang X, Zhao Y, Qian Y, Zhang, Li Q (2019) Recent Third Pole's Rapid Warming Accompanies Cryospheric Melt and Water Cycle Intensification and Interactions between Monsoon and Environment: Multidisciplinary Approach with Observations, Modeling, and Analysis. *Bulletin of the American Meteorological Society*, 100, 423–444

You Q, Wu T, Shen L, Pepin N, Zhang L, Jiang Z, Wu Z, Kang S, AghaKouchak A (2020) Review of snow cover variation over the Tibetan Plateau and its influence on the broad climate system. Earth-Science Reviews,201

Zhang T (2005) Influence of the seasonal snow cover on the ground thermal regime: An overview.Reviews of Geophysics,43

Zhao Y, Zhou T (2019) Asian water tower evinced in total column water vapor: a comparison among multiple satellite and reanalysis data sets. Clim Dyn 54:231–245